PHYSICAL REVIEW E **94**, 061102(R) (2016)

Coupled continuous-time random walks for fluid stretching in two-dimensional heterogeneous media

Marco Dentz*
Spanish National Research Council (IDAEA-CSIC), 08034 Barcelona, Spain

Daniel R. Lester
School of Engineering, RMIT University, 3000 Melbourne, Victoria, Australia

Tanguy Le Borgne
Geosciences Rennes, UMR 6118, Université de Rennes 1, CNRS, Rennes, France

Felipe P. J. de Barros
Sonny Astani Department of Civil and Environmental Engineering, University of Southern California, 3620 South Vermont Avenue, KAP 224B, Los Angeles, California 90089, USA

(Received 15 January 2016; published 27 December 2016)

We study the relation between flow structure and fluid deformation in steady flows through two-dimensional heterogeneous media, which are characterized by a broad spectrum of stretching behaviors, ranging from sub- to superlinear. We analyze these behaviors from first principles, which uncovers intermittent shear events to be at the origin of subexponential stretching. We derive explicit expressions for Lagrangian deformation and demonstrate that stretching obeys a coupled continuous-time random walk, which for broad distributions of flow velocities becomes a Lévy walk. The derived model provides a direct link between the flow and deformation statistics, and a natural way to quantify the impact of intermittent shear events on the stretching behavior.

DOI: 10.1103/PhysRevE.94.061102

I. INTRODUCTION

The deformation dynamics and stretching history of material fluid elements are fundamental for the understanding of hydrodynamic phenomena ranging from scalar dispersion, pair dispersion [1–3], mixing [4–9] and reaction [10–13] to the alignment of material elements [14], and the distribution of stress in complex fluids [15]. Fluid elements constitute the Lagrangian support of a transported scalar. Thus, their deformation histories determine the organization of the scalar distribution into lamellar structures [16–19]. Observed broad scalar concentration distributions are a manifestation of a broad distribution of stretching and compression rates and can explain intermittent patterns of scalar increment distributions [16,17]. The temporal scaling of the average elongation $\langle \ell(t) \rangle$ of material lines controls the decay of scalar variance, the effective kinetics of chemical reactions, and the distribution of scalar gradients [20]. The mechanisms of linear stretching due to persistent shear deformation, and exponential stretching in chaotic flows have been well understood [20]. Observations of subexponential and nonlinear fluid elongation [19,21,22], pair dispersion [1–3,23,24], and scalar variance decay [25,26], however, challenge these paradigms and ask for new dynamic frameworks. As a consequence, different mechanisms of subexponential stretching have been proposed, including fractal or spiral mixing (see, e.g., Ref. [26]), nonsequential stretching (see, e.g., Ref. [22]), and modified Richardson laws (see, e.g., Ref. [25]). The dynamics of particle pair separation, for example, has been described using Lévy processes and continuous-time random walks [1,3,27]. Elongation time series for stretching in $d = 2$ dimensional heterogeneous porous media flows have been modeled as geometric Brownian motions [8]. Most stochastic stretching models, however, do not provide relations between the deformation dynamics and the local Lagrangian and Eulerian deformations and flow structure. This means the fluctuation mechanisms that cause observed algebraic stretching are often not known.

We focus here on fluid deformation in flows through heterogeneous porous media, which play a key role for the understanding of mixing and reaction processes in natural and engineered materials [28,29]. For such flows, the mechanisms of (anomalous) particle dispersion have been the subject of intense theoretical and experimental studies [30–42]. The mechanisms of fluid stretching, however, are much less known. Here, we study the relation between velocity fluctuations and fluid deformation in nonhelical steady flows through random media, specifically, we refer to steady $d = 2$ pore-scale and $d = 2$ and $d = 3$ dimensional Darcy-scale flows in heterogeneous media [28]. The Darcy equation, which governs flow through porous media, implies that helicity is 0 in $d = 3$ dimensions [43,44], and prohibits closed streamlines in $d = 2$ [45]. Thus, flows through heterogeneous porous media are characterized by open streamlines, along which fluid particles may sample the full velocity spectrum [32,46–48]. We derive here the mechanisms of subexponential and power-law stretching behaviors in such flows. To this end, we formulate Lagrangian deformation in streamline coordinates [49], which allows relating elongation to Lagrangian velocities and shear deformation from first principles. The consequences of this coupling are studied in the framework of a continuous-time random walk (CTRW) [36,50–52] that links

*marco.dentz@csic.es

transit times of material fluid elements to elongation through Lagrangian velocities. The CTRW framework has been used extensively for the quantification of particle motion in flows through heterogeneous media [36]. We develop here a CTRW framework to quantify the stretching of material fluid elements.

II. FLUID DEFORMATION

Our analysis starts with the equation of motion of a fluid particle in a steady spatially varying flow field. The particle position $\mathbf{x}(t|\mathbf{a})$ in the divergence-free flow field $\mathbf{u}(\mathbf{x})$ evolves according to the advection equation

$$\frac{d\mathbf{x}(t|\mathbf{a})}{dt} = \mathbf{v}(t), \tag{1}$$

where $\mathbf{v}(t) = \mathbf{u}[\mathbf{x}(t|\mathbf{a})]$ denotes the Lagrangian velocity. The initial condition is given by $\mathbf{x}(t = 0|\mathbf{a}) = \mathbf{a}$. The particle movement along a streamline can be formulated as

$$\frac{ds(t)}{dt} = v(t), \quad dt = \frac{ds}{v_s(s)}, \tag{2}$$

where $s(t)$ is the distance traveled along the streamline, $v(t) = |\mathbf{v}(t)|$, and the streamwise velocity is $v_s(s) = |\mathbf{v}[t(s)]|$. With these preparations, we focus now on the evolution of the elongation of an infinitesimal material fluid element, whose length and orientation are described by the vector $\mathbf{z}(t) = \mathbf{x}(t|\mathbf{a} + \delta\mathbf{a}) - \mathbf{x}(t|\mathbf{a})$. According to (1), its evolution is governed by

$$\frac{d\mathbf{z}(t)}{dt} = \boldsymbol{\epsilon}(t)\mathbf{z}(t), \tag{3}$$

where $\boldsymbol{\epsilon}(t) = \nabla\mathbf{u}[\mathbf{x}(t|\mathbf{a})]^\top = \nabla\mathbf{v}(t)^\top$ is the velocity gradient tensor. Note that $\mathbf{z}(t) = \mathbf{F}(t)\mathbf{z}(0)$ with $\mathbf{F}(t)$ the deformation tensor. Thus, $\mathbf{F}(t)$ satisfies Eq. (3) and the following analysis is equally valid for the deformation tensor. The elongation $\ell(t)$ is given by $\ell(t) = |\mathbf{z}(t)|$. We transform the deformation process into the streamline coordinate system [49], which is attached to and rotates along the streamline described by $\mathbf{x}(t|\mathbf{a})$,

$$\mathbf{x}'(t) = \mathbf{A}^\top(t)[\mathbf{x}(t) - \mathbf{x}(t|\mathbf{a})], \tag{4}$$

where the orthogonal matrix $\mathbf{A}(t)$ describes the rotation operator which orients the x_1 coordinate with the orientation of velocity $\mathbf{v}(t)$ along the streamline such that $\mathbf{A}(t) = [\mathbf{v}(t), \mathbf{w}(t)]/v(t)$ with $\mathbf{w}(t) \cdot \mathbf{v}(t) = 0$ and $|\mathbf{w}(t)| = v(t)$. From this, we obtain for $\mathbf{z}'(t) = \mathbf{A}^\top\mathbf{z}(t)$ in the streamline coordinate system

$$\frac{d\mathbf{z}'(t)}{dt} = [\mathbf{Q}(t) + \tilde{\boldsymbol{\epsilon}}(t)]\mathbf{z}'(t), \tag{5}$$

where we defined $\tilde{\boldsymbol{\epsilon}}(t) = \mathbf{A}^\top(t)\boldsymbol{\epsilon}(t)\mathbf{A}(t)$ and the antisymmetric tensor $\mathbf{Q}(t) = \frac{d\mathbf{A}^\top(t)}{dt}\mathbf{A}(t)$. Thus, the velocity gradient tensor $\boldsymbol{\epsilon}(t)$ transforms into the streamline system as $\boldsymbol{\epsilon}'(t) = \mathbf{Q}(t) + \tilde{\boldsymbol{\epsilon}}(t)$. A quick calculation reveals that the components of $\mathbf{Q}(t)$ are given by $Q_{12}(t) = -Q_{21}(t) = \tilde{\epsilon}_{21}(t)$, where we use that $\frac{d\mathbf{v}(t)}{dt} = \boldsymbol{\epsilon}(t)\mathbf{v}(t)$. This gives for the velocity gradient in the streamline system the upper triangular form

$$\boldsymbol{\epsilon}'(t) = \begin{bmatrix} \tilde{\epsilon}_{11}(t) & \sigma(t) \\ 0 & -\tilde{\epsilon}_{11}(t) \end{bmatrix}, \tag{6}$$

where we define the shear rate $\sigma(t) = \tilde{\epsilon}_{12}(t) + \tilde{\epsilon}_{21}(t)$ along the streamline. Note that $\tilde{\epsilon}_{11}(t) = dv_s[s(t)]/ds$ by definition. Furthermore, due to the incompressibility of $\mathbf{u}(\mathbf{x})$, $\tilde{\epsilon}_{22}(t) = -\tilde{\epsilon}_{11}(t)$. For simplicity of notation, in the following we drop the primes. The upper triangular form of $\boldsymbol{\epsilon}(t)$ permits an explicit solution of (5) and reveals the dynamic origins of algebraic stretching.

Thus, we can formulate the evolution equation (5) of a material strip in streamline coordinates as

$$dz_1(s) = \frac{dv_s(s)}{v_s(s)}z_1(s) + \frac{\sigma(s)}{v_s(s)}z_2(s)ds, \tag{7a}$$

$$dz_2(s) = -\frac{dv_s(s)}{v_s(s)}z_2(s), \tag{7b}$$

where we used (2) to express $\mathbf{z}(t) = \mathbf{z}[s(t)]$ in terms of the distance along the streamline. The system (7) can be integrated to [53]

$$z_1(s) = \frac{v_s(s)}{v_s(0)}\left[z_1(0) + z_2(0)\int_0^s ds'\sigma(s')\frac{v_s(0)^2}{v_s(s')^3}\right], \tag{8a}$$

$$z_2(s) = \frac{v_s(0)}{v_s(s)}z_2(0). \tag{8b}$$

Note that the deformation tensor $\mathbf{F}(t)$ in the streamline system has also an upper triangular form. Its components can be directly read off the system (8). The angle of the strip $\mathbf{z}(t)$ with respect to the streamline orientation is denoted by $\phi(t)$ such that $z_1(t) = \ell(t)\cos[\phi(t)]$ and $z_2(t) = \ell(t)\sin[\phi(t)]$. The strip length is given by $\ell(t) \equiv \ell[s(t)]$ with $\ell(s) = [z_1(s)^2 + z_2(s)^2]^{1/2}$.

The system (8) is of general validity for $d = 2$ dimensional steady flow fields. It reveals the mechanisms that lead to an increase of the strip elongation, which is fully determined by the shear deformation $\sigma(s)$ and the velocity $v_s(s)$ along the streamline. For a strip that is initially aligned with the streamline, $z_2(0) = 0$, the elongation is $\ell(s) = z_2(0)v_s(s)/v_s(0)$ because $z_2(s) \equiv 0$ remains zero. This means $\ell(s)$ merely fluctuates without a net increase [53]. Only if the strip is oriented away from the streamline can the streamwise velocity fluctuations be converted into stretching. This identifies the integral term in (8a) as the dominant contribution to the strip elongation. It represents the interaction of shear deformation and velocity with a linear contribution from the shear rate and a nonlinear contribution from velocity as $1/v_s(s)^3$, which may be understood as follows. One power comes from the divergence of streamlines in low velocity zones, which increases $z_2(s)$ and thus leads to enhanced shear deformation. The second power is purely kinematic due to the weighting with the residence time in a streamline segment. The third power stems from the fact that shear deformation in low velocity segments is applied while the strip is compressed in streamline direction. This deformation is then amplified as the strip is stretched due to velocity increase. As a result of this nonlinear coupling, the history of low velocity episodes has a significant impact on the net stretching as quantified by the integral term in (8b). This persistent effect is superposed with the local velocity fluctuations. These mechanisms are illustrated in Fig. 1. While for a stratified flow field with $\mathbf{u}(\mathbf{x}) = \mathbf{u}(x_2)$ velocity and shear

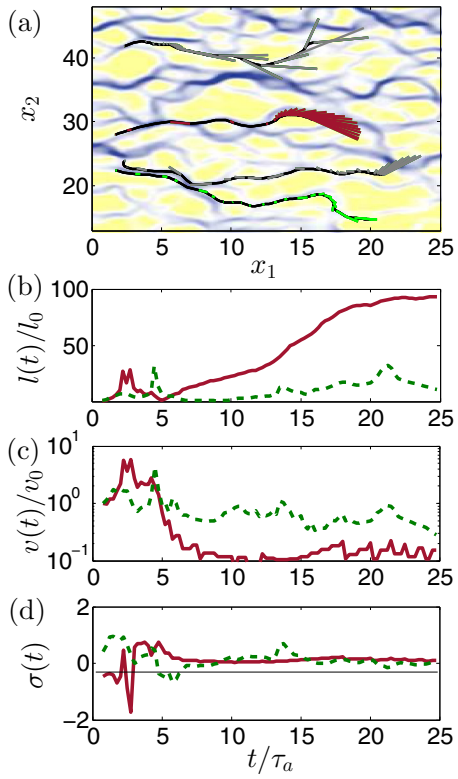

FIG. 1. (a) Illustration of the evolution of length (rescaled) and orientation of material strips along streamlines in a steady $d = 2$ dimensional divergence-free random flow [19]. The color scales illustrate the velocity magnitude decreasing from blue to yellow. Strips are drawn along streamlines at equidistant times. We observe persistent stretching in low velocity zones. This is reflected in the bottom panels, which illustrate (b) strip elongations $\ell(t)$ for two distinct streamlines characterized by high (green dashed) and low (red solid) velocities, (c) strip velocity time series, and (d) shear deformation corresponding to the strip evolutions illustrated in the left panel by the same colors.

deformation are constant along a streamline such that $\ell(t) = \{[z_1(0) + z_2(0)\sigma t]^2 + z_2(0)^2\}^{1/2}$, that is, it increases linearly with time, stretching can in general be sub- or superlinear, depending on the duration of low velocity episodes. In the following, we will analyze these behaviors in order to identify and quantify the origins of algebraic stretching.

III. DEFORMATION CTRW

To investigate the consequences of the nonlinear coupling between shear and velocity on the emergence of subexponential stretching, we cast the dynamics (8) in the framework of a CTRW for the Lagrangian flow velocities $v_s(s)$ [48]. Thus, we assume that the random flow field is stationary and ergodic [54]. Furthermore, we assume Lagrangian ergodicity [55], which means that fluid elements can sample the full velocity spectrum along a streamline [56]. As outlined in the Introduction, flow through heterogeneous porous media are in general characterized by open streamlines so that fluid particles can sample the full velocity spectrum as they move along a trajectory. This is not the case for flows in stratified media, in which velocities are perfectly correlated. Thus, here we consider random flows $\mathbf{u}(\mathbf{x})$ whose velocities fluctuations are controlled by a characteristic correlation length scale and focus on the impact of broad velocity point distributions rather than on that of long range correlations [30,57]. This is particularly relevant for porous media flows. It has been observed at the pore and Darcy scales that the streamwise velocity, that is, the velocity measured equidistantly along a streamline, follows a Markov process [38,40,41,46,58]. Thus, if we choose a coarse-graining scale that is of the order of the streamwise correlation length λ_c, (2) can be discretized as

$$s_{n+1} = s_n + \lambda_c, \quad t_{n+1} = t_n + \frac{\lambda_c}{v_n}. \tag{9}$$

The $v_n = v_s(s_n)$ are identical independently distributed random velocities with the probability density function (PDF) $p_v(v)$. A result of this spatial Markovianity is that the particle movement follows a continuous-time random walk (CTRW) [32,51]. The PDF of streamwise velocities $p_v(v)$ is related to the Eulerian velocity PDF $p_e(v)$ through flux weighting [48] as $p_v(v) \propto v p_e(v)$. The Eulerian velocity PDF in $d = 2$ dimensional pore networks, for example, can be approximated by a Gaussian-shaped distribution, which breaks down for small velocities [59]. For Darcy-scale porous and fractured media the velocity PDF can be characterized by algebraic behaviors at small velocities [32,41,60], which implies a broad distribution of transition times $\tau_n = \lambda_c/v_n$. Note, however, that the proposed CTRW stretching mechanisms are of a general nature and valid for any velocity distribution $p_v(v)$. In order to extract the deformation dynamics, we coarse-grain the elongation process along the streamline on the correlation scale λ_c. This gives for the strip coordinates (8)

$$z_1(s_n) = z_1(0)\frac{v_n}{v_0} + z_2(0)\frac{v_n v_0}{v_c^2}\sigma_c \tau_v r_n, \tag{10a}$$

$$z_2(s_n) = z_2(0)\frac{v_0}{v_n}, \tag{10b}$$

with v_c and σ_c a characteristic velocity and shear rate, and $\tau_v = \lambda_c/v_c$ a characteristic advection time. The process r_n, which results from the integral term in (8a), describes the coupled CTRW

$$r_{n+1} = r_n + \frac{v_c^3}{\sigma_c}\frac{\sigma_n}{v_n^3}, \quad t_{n+1} = t_n + \frac{\lambda_c}{v_n}. \tag{11}$$

The elongation at time t is given by $\ell(t) = [z_1(s_{n_t})^2 + z_2(s_{n_t})^2]^{1/2}$, where $n_t = \sup(n|t_n \leqslant t)$. It is observed over several $2d$ flows that the shear rate may be related to the streamwise velocity as $\sigma_n = \xi_n \sigma_c (v_n/v_c)^{\hat{\alpha}}$ with $\hat{\alpha} \approx 1$, σ_c a characteristic shear rate, and ξ_n an identical independent random variable that is equal to ± 1 with equal probability. The average shear rate $\langle \sigma_n \rangle = 0$ due to the stationarity of the random flow field $\mathbf{u}(\mathbf{x})$. Thus, (11) denotes a coupled CTRW whose increments $\rho_n \equiv r_{n+1} - r_n$ are related to the transition times $\tau_n = \lambda_c/v_n$ as

$$\rho_n = \xi_n(\tau_n/\tau_v)^\alpha, \quad \alpha = 3 - \hat{\alpha}. \tag{12}$$

It has the average $\langle \rho_n \rangle = 0$ and absolute value $|\rho_n| = (\tau_n/\tau_v)^\alpha$. The joint PDF of the elongation increments ρ and transition times τ is then given by

$$\psi(\rho, \tau) = \tfrac{1}{2}\delta[|\rho| - (\tau/\tau_v)^\alpha]\psi(\tau), \tag{13}$$

where $\delta(\rho)$ denotes the Dirac delta distribution. The transition time PDF $\psi(\tau)$ is related to the streamwise velocity PDF $p_v(v)$ as $\psi(\tau) = \lambda_c \tau^{-2} p_v(\lambda_c/\tau)$.

IV. ALGEBRAIC STRETCHING

In the following, we consider a streamwise velocity PDF that behaves as $p_v(v) \propto (v/v_c)^{\beta-1}$ for v smaller than the characteristic velocity v_c. Such a power law is a model for the low end of the velocity spectra in disordered media [30] and porous media flows [36,39,41]. Note, however, that the derived CTRW-based deformation mechanism is valid for any velocity distribution. The relation between the streamwise and Eulerian velocity PDFs, $p_v(v) \propto v p_e(v)$, implies that $\beta \geqslant 1$ because $p_e(v)$ needs to be integrable in $v = 0$. The corresponding transition time PDF $\psi(\tau)$ behaves as $\psi(\tau) \propto (\tau/\tau_v)^{-1-\beta}$ for $\tau > \tau_v = \lambda_c/v$ and decreases sharply for $\tau < \tau_v$. Due to the constraint $\beta > 1$, the mean transition time $\langle\tau\rangle < \infty$ is always finite, which is a consequence of fluid mass conservation. For transport in highly heterogeneous pore Darcy-scale porous media, values for β between 0 and 2 have been reported [36,39]. It has been found that decreasing medium heterogeneity leads to a sharpening of the transition time PDF and increase of the exponent β [41] with $\beta > 1$. With these definitions, the coupled CTRW (11) describes a Lévy walk.

Figure 2 shows the evolution of the average elongation $\langle\ell(t)\rangle$ for $\alpha = 2$ and different values of β obtained from numerical Monte Carlo simulations using (10) and the Lévy walk (11) for the evolution of the strip coordinates based on a gamma PDF of streamwise velocities [53]. The mean

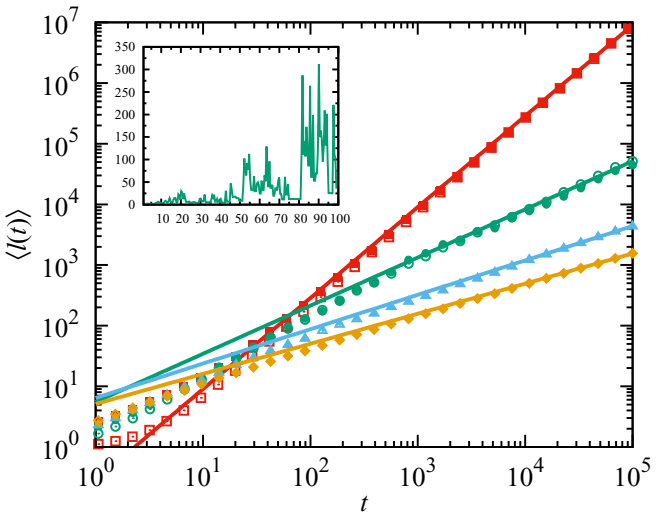

FIG. 2. Evolution of the (open symbols) mean elongation $\langle\ell(t)\rangle = \langle[z_1(s_{n_t})^2 + z_2(s_{n_t})^2]^{1/2}\rangle$ with ℓ_n given obtained from numerical Monte Carlo simulations using (10) and (11) for a uniform distribution of initial strip orientations $\phi \in [-\pi/2, \pi/2]$, $\alpha = 2$ and a gamma PDF of streamwise velocity. The solid symbols are obtained from the approximation (14) for (squares) $\beta = \frac{3}{2}$, (circles) $\beta = \frac{5}{2}$, (triangles) $\beta = \frac{7}{2}$, and (rhombi) $\beta = \frac{9}{2}$. The solid lines indicate the late time power-law behaviors of $\langle\ell(t)\rangle \propto t^{3-\beta}$ for $1 < \beta < 2$, $\langle\ell(t)\rangle \propto t^{2/\beta}$ for $2 < \beta < 4$, and $\langle\ell(t)\rangle \propto t^{1/2}$ for $\beta > 4$. The inset illustrates the evolution of $\ell(t)$ in a single realization of v_n for $\beta = \frac{5}{2}$ for an initial orientation of $\phi = 0$.

elongation shows a power-law behavior and increases as $\langle\ell(t)\rangle \propto t^{\nu}$. As discussed above, long episodes of small velocity maintain the strip in a favorable shear angle, which leads to a strong stretching. These dynamics are quantified by the Lévy walk process (11), which relates strong elongations to long transition times, i.e., small streamwise velocities, through (12). This is also illustrated in the inset of Fig. 2, which shows the elongation of a single material strip. The elongation events increase with increasing time as a consequence of the coupling (12) between stretching and transition time. This is an intrinsic property of a CTRW characterized by a broad $\psi(\tau)$; the transition times increase as time increases, and thus, through the Lévy walk coupling, also the stretching increments. In fact, the strip length can be approximated by [53]

$$\ell(t) \approx \ell_0 + \frac{\sigma_c \tau_v^2 \langle v\rangle}{\langle\tau\rangle v_c} |z_2(0)||r_{n_t}|. \tag{14}$$

The leading behavior of the mean elongation $\langle\ell(t)\rangle$ of a material element is directly related to the mean absolute moment of $r(t)$ as $\langle\ell(t)\rangle \propto \langle|r_{n_t}|\rangle$. Thus, even though r_{n_t} is in average 0, the addition of large elongation events in its absolute value $|r(t)|$, which correspond to episodes of low velocities, leads in average to an algebraic increase of $\ell(t)$ as detailed in the following.

The statistics of the Lévy walk (11) have been analyzed in detail in Ref. [61] for $\alpha > 0$ and $\beta > 0$. Here, β is restricted to $\beta > 1$ due to fluid mass conservation. Furthermore, we consider $\alpha \geqslant 1$. The scaling of the mean absolute moments of r_{n_t} depends on the α and β regimes.

If the exponent $\beta > 2\alpha$, which means relatively weak heterogeneity, we speak of weak coupling between the elongation increment ρ_n and the transition time τ_n in (12). In this case, the strip elongation behaves as $\langle\ell(t)\rangle \propto t^{1/2}$. We term this behavior here diffusive or normal stretching. For $\alpha = 2$ as employed in the numerical simulations this means that $\beta > 4$. The coupled Lévy walk (11) reduces essentially to a Brownian motion because the variability of transition times is low so that the coupling does not lead to strong elongation events. Note that scalar dispersion in this β range is normal [36,51].

For strong coupling, this means $\beta < 2\alpha$ and thus stronger flow heterogeneity, it has been shown [61] that the density of r_{n_t} is characterized by two scaling forms, one that characterizes the bulk behavior and a different one for large r_{n_t}. As a consequence, we need to distinguish the cases of β larger and smaller than α. Also, the scaling of $|r_{n_t}|$ cannot be obtained by dimensional analysis. In fact, r_{n_t} has a strong anomalous diffusive character [61].

For $\alpha < \beta < 2\alpha$ the scaling behavior of the mean elongation is $\langle\ell(t)\rangle \propto t^{\alpha/\beta}$. This means for $\alpha = 2$, the stretching exponent ν is between $\frac{1}{2}$ and 1, the β range is $2 < \beta < 4$. It interesting to note that scalar dispersion in this range is normal as well. Here, the frequency of low velocity regions is high enough to increase stretching above the weakly coupled case, but not to cause superdiffusive scalar dispersion.

For $1 < \beta < \alpha$ in contrast, the mean elongation scales as [61] $\langle\ell(t)\rangle \propto t^{1+\alpha-\beta}$. The stretching exponent is between 1 and α, and this means stretching is stronger than for shear flow. The range of scaling exponents ν of the mean elongation

here is $\frac{1}{2} \leqslant \nu < \alpha$. Specifically, $\alpha = 2$ implies that stretching is superlinear for $1 < \beta < 2$, and this means faster than by a pure shear flow, for which $\nu = 1$. Here, the presence of low velocities in the flow leads to enhanced stretching and at the same time to superdiffusive scalar dispersion.

V. SUMMARY AND CONCLUSIONS

In summary, we have presented a fundamental mechanism for power-law stretching in random flows through intermittent shear events, which may explain algebraic mixing processes observed across a range of heterogeneous flows. We have shown that the nonlinear coupling between streamwise velocities and shear deformation implies that stretching follows a coupled CTRW, which explains observed subexponential stretching behaviors that can range from diffusive to superdiffusive scalings, $\langle \ell(t) \rangle \propto t^{\nu}$ with $\frac{1}{2} \leqslant \nu < 2$. The derived coupled stretching CTRW can be parametrized in terms of the Eulerian velocity and deformation statistics and provides a link between anomalous dispersion and fluid deformation. The presented analysis demonstrates that the dynamics of fluid stretching in heterogeneous flow fields is much richer than the paradigmatic linear and exponential behaviors. The fundamental mechanism of intermittent shear events, which is at the root of nonexponential stretching, is likely present in a broader class of fluid flows.

ACKNOWLEDGMENTS

M.D. acknowledges the support of the European Research Council (ERC) through the project MHetScale (Contract No. 617511). T.L.B. acknowledges Agence National de Recherche (ANR) funding through Project No. ANR-14-CE04-0003-01.

[1] M. F. Shlesinger, B. J. West, and J. Klafter, Phys. Rev. Lett. **58**, 1100 (1987).
[2] M. P. Rast and J.-F. Pinton, Phys. Rev. Lett. **107**, 214501 (2011).
[3] S. Thalabard, G. Krstulovic, and J. Bec, J. Fluid Mech. **755**, R4 (2014).
[4] N. Kleinfelter, M. Moroni, and J. H. Cushman, Phys. Rev. E **72**, 056306 (2005).
[5] E. Villermaux and J. Duplat, Phys. Rev. Lett. **97**, 144506 (2006).
[6] B. Jha, L. Cueto-Felgueroso, and R. Juanes, Phys. Rev. Lett. **106**, 194502 (2011).
[7] F. P. J. de Barros, M. Dentz, J. Koch, and W. Nowak, Geophys. Res. Lett. **39**, L08404 (2012).
[8] T. Le Borgne, M. Dentz, and E. Villermaux, J. Fluid Mech. **770**, 458 (2015).
[9] Y. Ye, G. Chiogna, O. A. Cirpka, P. Grathwohl, and M. Rolle, Phys. Rev. Lett. **115**, 194502 (2015).
[10] W. E. Ranz, AIChE J. **25**, 41 (1979).
[11] A. M. Tartakovsky, D. M. Tartakovsky, and P. Meakin, Phys. Rev. Lett. **101**, 044502 (2008).
[12] N. B. Engdahl, D. A. Benson, and D. Bolster, Phys. Rev. E **90**, 051001(R) (2014).
[13] J. J. Hidalgo, M. Dentz, Y. Cabeza, and J. Carrera, Geophys. Res. Lett. **42**, 6357 (2015).
[14] G. Lapeyre, P. Klein, and P. L. Hua, Phys. Fluids **11**, 3729 (1999).
[15] C. Truesdell and W. Noll, *The Nonlinear Field Theories of Mechanics* (Springer, Berlin, 1992).
[16] J. Kalda, Phys. Rev. Lett. **84**, 471 (2000).
[17] E. Villermaux and J. Duplat, Phys. Rev. Lett. **91**, 184501 (2003).
[18] E. Villermaux, C. R. Mec. **340**, 933 (2012).
[19] T. Le Borgne, M. Dentz, and E. Villermaux, Phys. Rev. Lett. **110**, 204501 (2013).
[20] J. Ottino, *The Kinematics of Mixing: Stretching, Chaos, and Transport* (Cambridge University Press, Cambridge, UK, 1989).
[21] J. Duplat and E. Villermaux, Eur. Phys. J. B **18**, 353 (2000).
[22] J. Duplat, C. Innocenti, and E. Villermaux, Phys. Fluids **22**, 035104 (2010).
[23] S. Goto and J. C. Vassilicos, New J. Phys. **6**, 65 (2004).
[24] E. Afik and V. Steinberg, arXiv:1502.02818.
[25] M. Nelkin and R. M. Kerr, Phys. Fluids **24**, 1754 (1981).
[26] J. C. Vassilicos, Philos. Trans. R. Soc., A **360**, 2819 (2002).
[27] G. Boffetta and I. M. Sokolov, Phys. Rev. Lett. **88**, 094501 (2002).
[28] J. Bear, *Dynamics of Fluids in Porous Media* (American Elsevier, New York, 1972).
[29] H. Brenner and D. A. Edwards, *Macrotransport Processes* (Butterworth-Heinemann, Oxford, UK, 1993).
[30] J. P. Bouchaud and A. Georges, Phys. Rep. **195**, 127 (1990).
[31] J. H. Cushman, X. Hu, and T. R. Ginn, J. Stat. Phys. **75**, 859 (1994).
[32] B. Berkowitz and H. Scher, Phys. Rev. Lett. **79**, 4038 (1997).
[33] D. A. Benson, S. W. Wheatcrat, and M. M. Meerschaert, Water Resour. Res. **36**, 1403 (2000).
[34] R. Haggerty, S. A. McKenna, and L. C. Meigs, Water Resour. Res. **36**, 3467 (2000).
[35] J. D. Seymour, J. P. Gage, S. L. Codd, and R. Gerlach, Phys. Rev. Lett. **93**, 198103 (2004).
[36] B. Berkowitz, A. Cortis, M. Dentz, and H. Scher, Rev. Geophys. **44**, RG2003 (2006).
[37] S. P. Neuman and D. M. Tartakovsky, Adv. Water Resour. **32**, 670 (2008).
[38] T. Le Borgne, M. Dentz, and J. Carrera, Phys. Rev. Lett. **101**, 090601 (2008).
[39] B. Bijeljic, P. Mostaghimi, and M. J. Blunt, Phys. Rev. Lett. **107**, 204502 (2011).
[40] P. De Anna, T. Le Borgne, M. Dentz, A. M. Tartakovsky, D. Bolster, and P. Davy, Phys. Rev. Lett. **110**, 184502 (2013).
[41] Y. Edery, A. Guadagnini, H. Scher, and B. Berkowitz, Water Resour. Res. **50**, 1490 (2014).
[42] A. Tyukhova, M. Dentz, W. Kinzelbach, and M. Willmann, Phys. Rev. Fluids **1**, 074002 (2016).
[43] G. Sposito, Water Resour. Res. **30**, 2395 (1994).
[44] G. Sposito, Adv. Water Resour. **24**, 793 (2001).
[45] M. Dentz, H. Kinzelbach, S. Attinger, and W. Kinzelbach, Phys. Rev. E **67**, 046306 (2003).
[46] T. Le Borgne, M. Dentz, and J. Carrera, Phys. Rev. E **78**, 026308 (2008).

[47] V. Cvetkovic, A. Fiori, and G. Dagan, Water Resour. Res. **50**, 5759 (2014).
[48] M. Dentz, P. K. Kang, A. Comolli, T. Le Borgne, and D. R. Lester, Phys. Rev. Fluids **1**, 074004 (2016).
[49] H. Winter, J. Non-Newtonian Fluid Mech. **10**, 157 (1982).
[50] E. W. Montroll and G. H. Weiss, J. Math. Phys. **6**, 167 (1965).
[51] H. Scher and M. Lax, Phys. Rev. B **7**, 4491 (1973).
[52] A. Zaburdaev, S. Denisov, and J. Klafter, Rev. Mod. Phys. **87**, 483 (2015).
[53] See Supplemental Material at http://link.aps.org/supplemental/10.1103/PhysRevE.94.061102 for details on the derivation of the equations for the strip deformation in the streamline coordinate system, the approximations for the calculation of the average strip elongation, and the numerical random walk particle tracking simulations.
[54] G. Christakos, *Random Field Models in Earth Sciences* (Academic, New York, 1992).
[55] A. M. Yaglom, *An Introduction to the Theory of Stationary Random Functions* (Dover, New York, 1962).
[56] For random flows displaying open and closed streamlines such as the steady $d = 2$ dimensional Kraichnan model, we focus on stretching in the subset of ergodic streamlines. Stretching due to shear on closed streamlines is linear in time.
[57] M. Dentz and D. Bolster, Phys. Rev. Lett. **105**, 244301 (2010).
[58] P. K. Kang, M. Dentz, T. Le Borgne, and R. Juanes, Phys. Rev. Lett. **107**, 180602 (2011).
[59] A. D. Araújo, W. B. Bastos, J. S. Andrade, and H. J. Herrmann, Phys. Rev. E **74**, 010401(R) (2006).
[60] P. K. Kang, M. Dentz, T. Le Borgne, and R. Juanes, Phys. Rev. E **92**, 022148 (2015).
[61] M. Dentz, T. Le Borgne, D. R. Lester, and F. P. J. de Barros, Phys. Rev. E **92**, 032128 (2015).